Shielding Analysis for a Heavy Ion Beam Chamber with Plasma Channels for Ion Transport

M.E. Sawan, R.R. Peterson, S. Yu

September 1999

UWFDM-1105

Presented at the 5th International Symposium on Fusion Nuclear Technology, Rome, Italy, 19-24 September 1999

Shielding Analysis for a Heavy Ion Beam Chamber with Plasma Channels for Ion Transport

M.E. Sawan, R.R. Peterson, S. Yu[1]

Fusion Technology Institute
Department of Engineering Physics
University of Wisconsin-Madison
1500 Engineering Drive
Madison, WI 53706

September 1999

UWFDM-1105

Presented at the 5th International Symposium on Fusion Nuclear Technology, Rome, Italy, 19-24 September 1999.

---

[1] Lawrence Berkeley National Laboratory, University of California, Berkeley, CA 94720

Abstract

Neutronics analysis has been performed to assess the shielding requirements for the insulators and final focusing magnets in a modified HYLIFE-II target chamber that utilizes pre-formed plasma channels for heavy ion beam transport. Using 65 cm thick Flibe jet assemblies provides adequate shielding for the electrical insulator units. Additional shielding is needed in front of the final focusing superconducting quadrupole magnets. A shield with a thickness varying between 45 and 90 cm needs to be provided in front of the quadrupole unit. The final laser mirrors located along the channel axis are in the direct line-of-sight of source neutrons. Neutronics calculations were performed to determine the constraints on the placement of these mirrors to be lifetime components.

1. Introduction

Ion transport in pre-formed plasma channels has been considered as a possible attractive option for ion beam fusion power plants. A point design of a final focus and reactor system, shown in Fig. 1, has been developed [1]. The target chamber considered is based on a modified HYLIFE-II reactor [2].

In this concept, thick curtains of Flibe are employed to protect the chamber wall from neutrons generated in the target. Three Flibe jet assemblies are injected into the chamber forming a neutronically thick layer between the burning target and the first wall. Each assembly has a thickness of 50 cm. These jets are arranged alternatively in horizontal and vertical directions. Each jet assembly has a 6 cm wide slot. The slots in the jet assemblies serve to define the 6 cm x 6 cm penetration for the pre-formed plasma channels used for ion beam transport to the target. The impact of neutron streaming through these penetrations on the sensitive components of the beam transport system is analyzed. This system includes insulators to prevent electrical breakdown between the channels and the target chamber wall, an adiabatic lens to focus the ion beams into the channels, a set of superconducting focusing magnets, and an optics system for lasers that guides the paths of the channels. Neutronics analysis has been performed to assess the shielding requirements and determine damage level in these components.

While most of the magnets and electrical insulators will be in the shadow of the full 150 cm thick Flibe jets, parts of them will be shielded by only 100 cm or 50 cm of Flibe due to the arrangement of the slots in the Flibe jets. Several conservative one-dimensional (1-D) calculations were performed to determine the shielding requirements at these hot spots. In addition, the final laser optics will be exposed to direct streaming source neutrons. The placement of the laser metallic mirrors relative to the target was determined to allow them to be lifetime components. The results presented here are normalized to a fusion power of 2580 MW (430 MJ target yield at 6 Hz) and 30 full power years (FPY) of operation.

2. Electrical insulator shielding

Ceramic insulators are used to provide electrical insulation in the adiabatic lens and between the channel and the chamber. Candidate materials include Al_2O_3, MgO, and spinel ($MgAl_2O_4$). In a nuclear environment, degradation of electrical and mechanical properties of the insulator is the main concern [3]. Neutron damage has no effect on the strength of the compacted powder ceramics since each grain is affected individually. However, the mechanical and structural degradation in polycrystalline solid insulators used in this design depends on the crystal structure. The non-cubic materials such as Al_2O_3 swell anisotropically leading to the onset of structural microcracking even at modest fluences [4]. On the other hand, swelling in solid ceramics with cubic structure (e.g. MgO and $MgAl_2O_4$) is isotropic under neutron irradiation [5]. In fact, the fracture toughness of these materials actually increases under elevated neutron fluences [5]. Therefore, the fluence limit for cubic ceramics is determined only by the maximum swelling to be tolerated. In this study, a maximum swelling of 3% is considered. This corresponds to fast neutron ($E > 0.1$ MeV) fluences of 1.1×10^{22} and 4×10^{22} n/cm^2 for MgO and spinel, respectively [5]. Spinel is chosen in this study since it offers the lowest mechanical and structural degradation in a nuclear environment among its class of solid ceramic insulators.

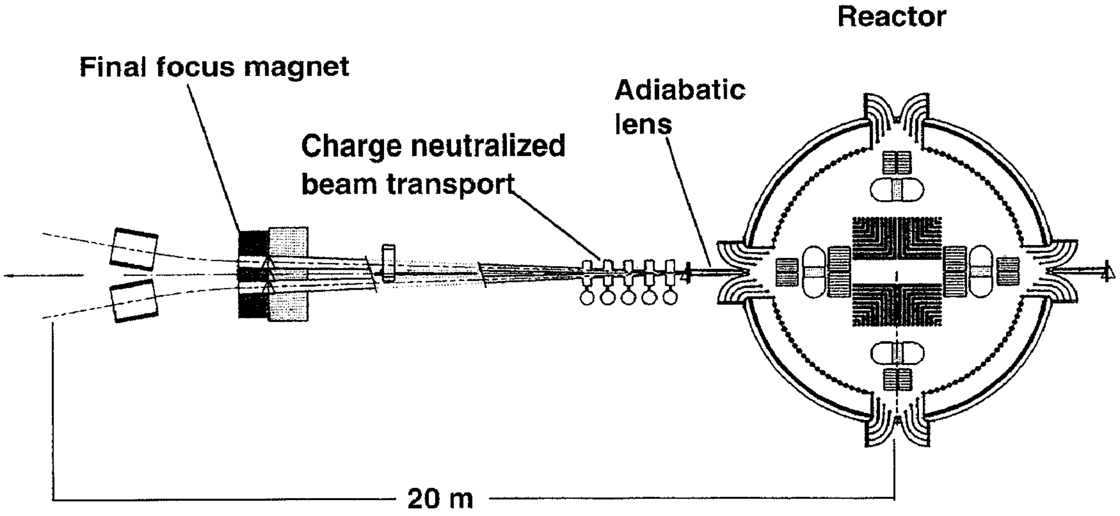

Fig. 1. Schematic of channel-based reactor/final transport system.

Under large instantaneous neutron and gamma dose rates, ceramic insulators exhibit a significant and instantaneous decrease in their electrical resistivity [4,6]. Such degradation in resistivity can lead to thermal runaway. This effect is lower in solid ceramics and is only important for very high dose rates. In addition, since the neutron pulse arrives at the insulator about 70 ns following the shot, the peak instantaneous dose rate occurs at a delayed time after the shot and the large resistivity of the insulator required at the time of the shot will not be affected.

Direct source neutrons streaming through the beam penetrations in the Flibe curtains will not affect the lifetime of the insulator between the channel and the chamber wall as long as a central opening at least 10 cm wide is used at the center of the insulator. The direct streaming neutrons will pass through without impinging on the insulator. In addition, since the conical insulator in the adiabatic lens has an inner radius ranging from 5 to 10 cm, the direct streaming neutrons do not affect it. Both electrical insulators are in the shadow of the Flibe jets relative to the direct source neutrons emitted from the target provided that these jet assemblies extend to at least 60 cm from the channel axis.

The insulator at the chamber wall is protected from the neutrons emitted from the target by the Flibe jets. While most of the insulator is protected by the full 150 cm, some hot spots are shielded by only 100 cm or 50 cm of Flibe. Several calculations were performed to determine the impact of the Flibe thickness on the fast neutron fluence in the insulator. Improving the shielding performance of the Flibe by enriching the Li in ^{6}Li, which is a good neutron absorber, was also assessed. Enriching the Li is expected to reduce tritium breeding in Flibe. However, this option was considered since the tritium breeding ratio is relatively high (1.255) with a comfortable margin for tritium self-sufficiency.

Figure 2 shows the variation of the peak insulator fast neutron fluence with Li enrichment for different Flibe thicknesses. It is clear that the impact of enrichment on improving the shielding performance is minimal. The resulting peak end-of-life fast neutron fluence is lower than the 4×10^{22} n/cm^2 design limit for Flibe thicknesses of 100 and 150 cm. This implies that most of the insulator and even the hot spots shielded by only 100 cm of Flibe will last for the whole reactor lifetime. On the other hand, parts of the insulator protected by only 50 cm of Flibe will experience a peak end-of-life fast neutron fluence of 1.3×10^{23} n/cm^2, which exceeds the design limit for maximum swelling of

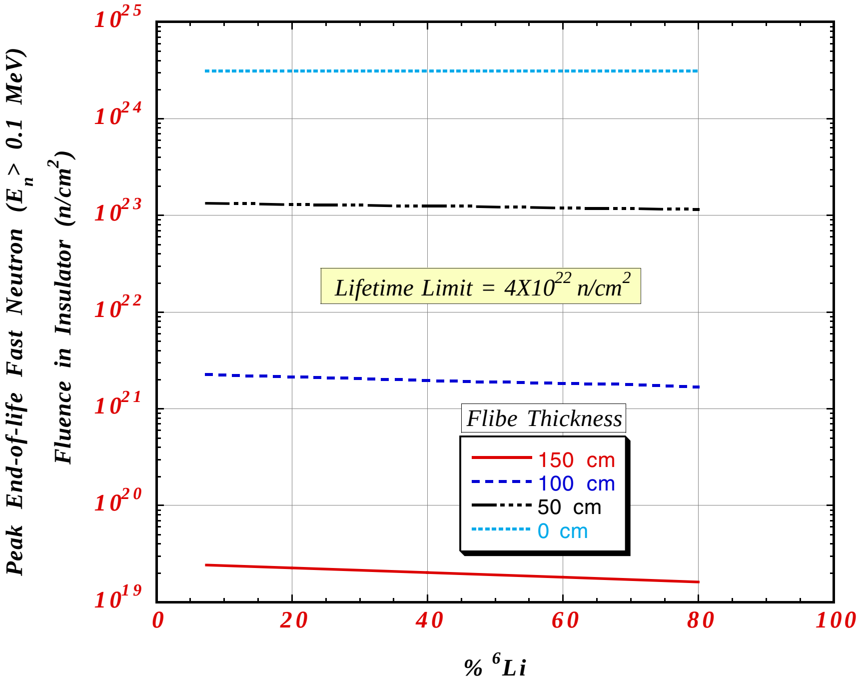

Fig. 2. Effect of Flibe thickness and enrichment on neutron fluence in the insulator.

3%. Local swelling at these hot spots is expected to be ~10%. The fast neutron fluence, and hence, the amount of swelling drops as one moves in the insulator away from the surface facing the target. The fluence drops by an order of magnitude in every 25 cm of the insulator. If the design can accommodate this amount of swelling at limited hot spots, the thickness of each Flibe jet assembly can be kept at 50 cm. Alternatively, the jet assembly thickness should be increased.

Figure 3 gives the minimum Flibe thickness required for the insulator to be a lifetime component. The results are given as a function of Li enrichment. A reduction of only 2.5 cm in the required thickness is achieved by enrichment. On the other hand, the tritium breeding ratio is reduced by 8%. Therefore, enriching the Li is not a viable solution. The results of Fig. 3 imply that using 65 cm thick jet assemblies will be adequate for protecting the insulator. Notice that these results are conservative since they are based on 1-D calculations with the target surrounded by the thin Flibe layer everywhere while in reality the thicker layers of Flibe elsewhere will reduce the contribution of secondary neutrons at the hot spots.

The insulator in the adiabatic lens is shielded from the source neutrons by the insulator at the chamber wall and the 10 cm steel electrode at the chamber side of the adiabatic lens in addition to the shielding provided by the Flibe jet assemblies. As a result, the peak neutron fluence in the adiabatic lens insulator is a factor of 70 lower than that in the insulator region at the chamber wall. Hence, even for the limited areas protected by only 50 cm of Flibe, the peak end-of-life fluence in the insulator of the adiabatic lens is only 1.9×10^{21} n/cm^2 implying that it is a lifetime component.

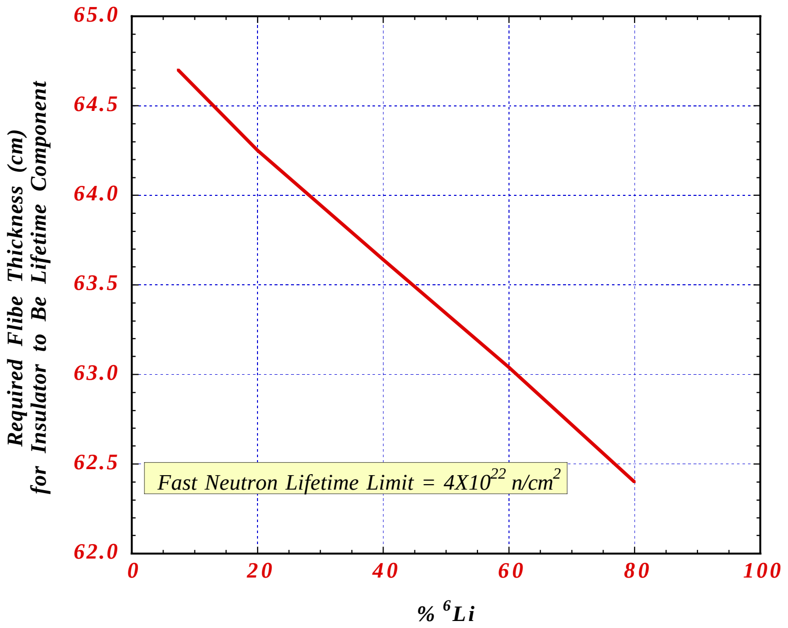

Fig. 3. Flibe thickness required for insulator protection as a function of lithium enrichment.

3. Shielding for final focusing magnets

The final superconducting quadrupole magnet in the ion beam final focusing system is located at 10 meters from the plasma adiabatic lens. Four superconducting coils surround the four ion beam tubes. At this location, the center of each of the four beam tubes with an inner radius of 15 cm is at 30 cm from the channel axis. A central penetration in this quadrupole assembly is used for passage of the laser beam. Adequate shielding should be provided to protect the superconducting magnets from neutrons emitted from the target. The superconducting coil composition is taken to be similar to the composition of the winding pack of the toroidal field coil of ITER [7]. It consists of 43.2% SS, 11.7% Cu, 2.9% Nb_3Sn, 7.4% Bronze, 16.8% liquid He, and 18% insulator (epoxy with 70% R-glass). The damage in the copper stabilizer should be limited because it results in a resistivity increase [8]. An end-of-life Cu dpa limit of 6×10^{-3} dpa is considered here. The dose limit for the organic electrical insulator in the superconducting magnet is determined by the requirement that the insulator retains at least 75% of its mechanical strength [8]. For the glass-fiber-filled epoxy this limit is 10^9 rads. A fast neutron fluence limit of 10^{19} n/cm^2 is used here. Currently available irradiation data indicate that this fluence will not result in significant degradation of the critical properties of Nb_3Sn [8]. The limit on peak magnet nuclear heating is taken to be 1 mW/cm^3. These radiation limits are similar to those adopted in ITER [7].

The central part of the quadrupole unit up to a radius of 5 cm is exposed to direct streaming source neutrons. A conical penetration with the inner surface inclined along the direct line-of-sight of source neutrons should be employed to eliminate any of the direct source neutrons from impinging on the quadrupole assembly and contributing to magnet damage. This approach was found to significantly reduce the shielding requirement for the final focusing magnets of heavy ion beam driven plants [9]. The part of the final quadrupole assembly within a radius ranging from 5 cm to 17 cm is protected from source neutrons by the 15 cm total thickness of the steel electrodes of the adiabatic lens. Additional shielding is needed in front of the quadrupole assembly in this region. A shield consisting of 70% SS and 30% water was considered. The effect of shield thickness on magnet radiation effects was determined. The insulator dose limit was found to be the most limiting parameter that determines the shielding requirement. An incremental shield thickness of 17.3 cm decreases the insulator dose by an order of magnitude. Based on this analysis a shield thickness of 90 cm is required.

The part of the quadrupole assembly at a radius larger than 46 cm is protected from the source neutrons by the Flibe jets and the 35 cm thick electrical insulator at the chamber wall. While most of this part of the quadrupole assembly is protected by the full 150 cm of Flibe, some hot spots are shielded by only 100 cm or 50 cm of Flibe. Several calculations were performed to determine the impact of the Flibe thickness on the amount of additional shielding required. Figure 4 gives the variation of the peak end-of-life magnet insulator dose with the thickness of additional steel/water shield. The results are given for different thicknesses of the Flibe in the chamber. While no additional shielding is required for parts of the magnets in the shadow of the full 150 cm thick Flibe jets, additional shielding is required at azimuthal locations with less Flibe protection. For jet assemblies that are 50 cm thick each, an additional 45 cm thick shield is needed. This is a conservative estimate since the magnet is more than 12 m away from the Flibe jets and the impact of the 6 cm wide gaps in the jet assemblies on magnet damage peaking will be significantly diluted. In addition, no credit is taken for the additional shielding provided by the baffle chamber and pumping units located between the adiabatic lens and the final focusing magnets. A shield with a thickness decreasing linearly from 90 cm at 17 cm radius to 45 cm at 46 cm radius needs to be provided in front of the quadrupole unit as shown in Fig. 5. Penetrations should be provided in the shield to allow for passage of the ion beams. Multi-dimensional calculations are needed to confirm these results.

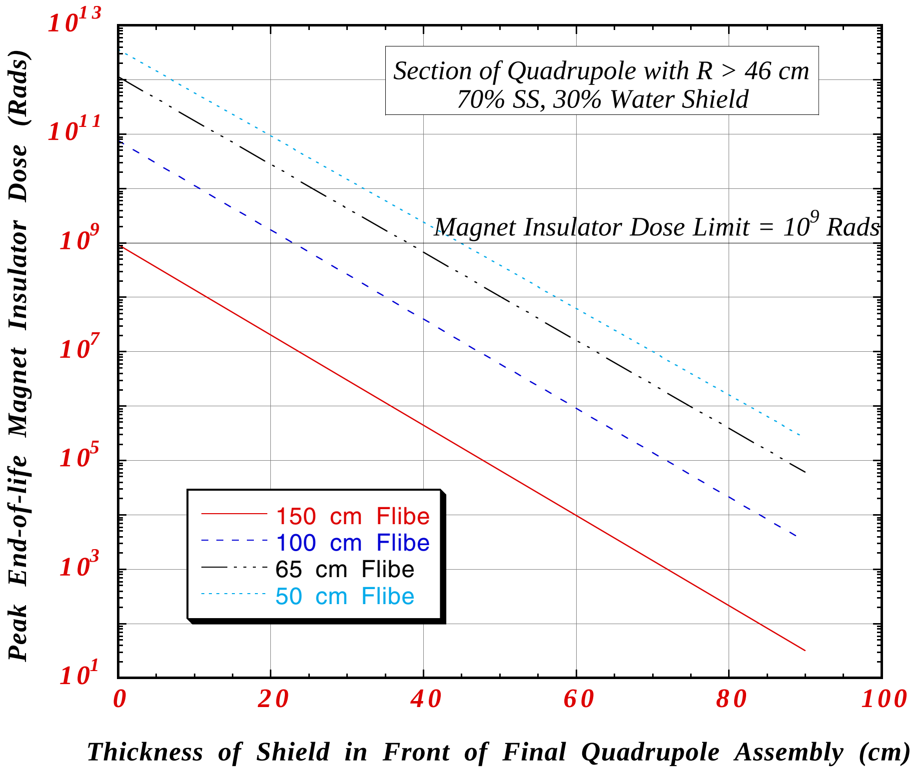

Fig. 4. Additional magnet shielding requirement.

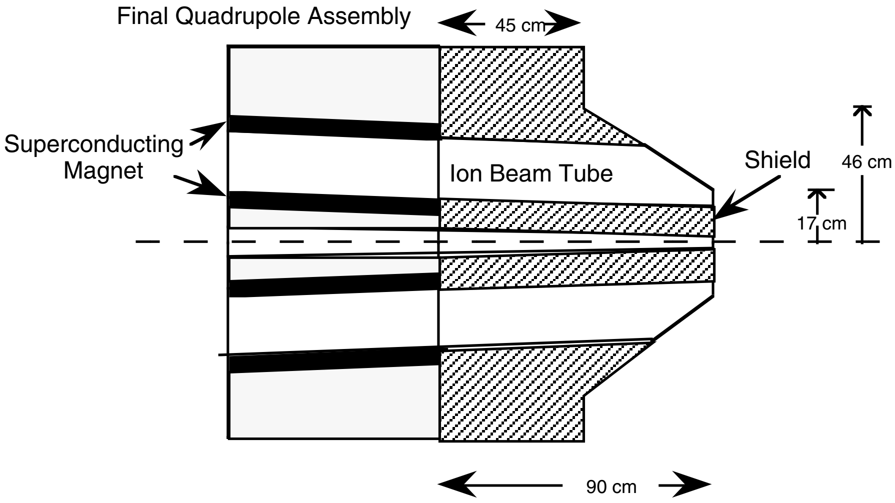

Fig. 5. Shield configuration for the final quadrupole assembly.

4. Placement of final laser mirrors

The lifetime of the final laser mirrors depends on the neutron fluence limit for the dielectric coated or metallic mirrors, damage recovery with annealing and the location of the mirror relative to the target. The final laser mirror located along the channel axis is in the direct line-of-sight of source neutrons and will experience the largest radiation damage. Dielectric coated mirrors are more sensitive to neutron radiation that degrades the optical transmission of the dielectric material, decomposes the dielectric materials, and destroys the interfaces between dielectric layers. Removing them from the line-of-sight of target neutrons can protect the sensitive dielectric mirrors. The more radiation resistant grazing incidence metallic mirrors (GIMM) are placed in the direct line-of-sight [10]. The lifetime of the GIMM is limited by mirror deformation from swelling and creep that leads to defocusing of the laser beam. A fraction of the neutron-produced damage can be recovered by annealing. There are very limited experimental data on radiation damage to metallic mirrors.

The fast neutron flux ($E > 0.1$ MeV) at the GIMM is given as a function of distance from the target, R (m), as $7.24 \times 10^{15}/R^2$ n/cm^{2}s and is contributed mostly by the direct source neutrons. Assuming no damage recovery with annealing, the lifetime is determined by dividing the fast neutron fluence limit by the fast neutron flux at the mirror. In order for the mirrors to last for the full 30 FPY of reactor operation, they have to be located at minimum distances from the target of 262, 83, or 26.2 m for fluence limits of 10^{20}, 10^{21}, and 10^{22} n/cm^2, respectively. If partial recovery is possible with annealing, the lifetime can be extended until the time between anneals becomes very small. A minimum time of one month between anneals is assumed. Figure 6 gives the minimum distance from the target for the metallic mirror to be a lifetime component. It is clear that the lifetime of the GIMM is very sensitive to the neutron fluence limit and damage recovery. Experimental data on radiation damage to metallic mirrors are essential to allow for a more accurate prediction of the GIMM lifetime.

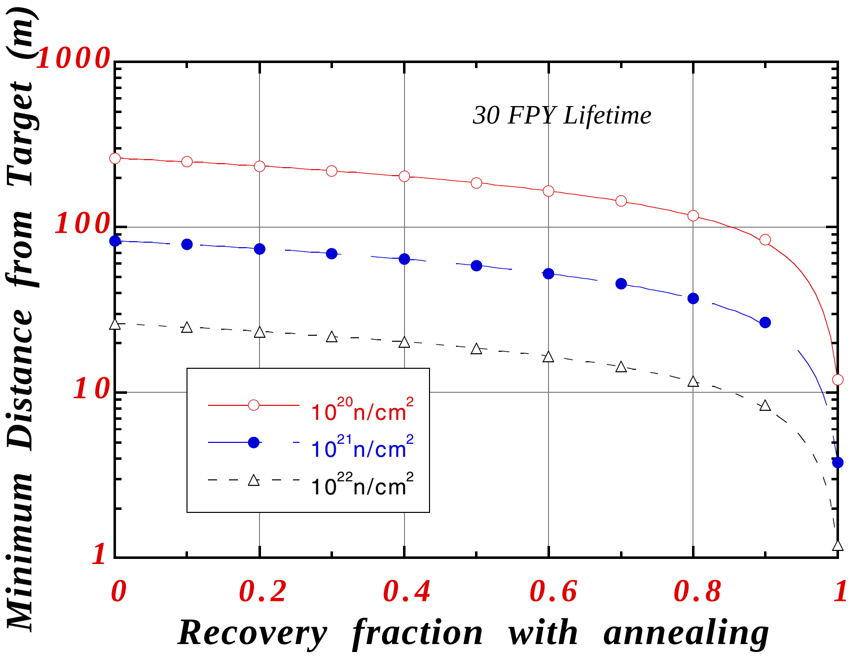

Fig. 6. Minimum distance of final metallic mirror from target as a function of fluence limit and fraction of recovery with annealing.

5. Summary and conclusions

Neutronics analysis has been performed to assess the shielding requirements for the insulators and final focusing magnets in a modified HYLIFE-II target chamber that utilizes pre-formed plasma channels for heavy ion beam transport. Thick curtains of Flibe are employed to protect the chamber wall from neutrons generated in the target. Spinel is chosen as insulator material since it offers the lowest mechanical and structural degradation in a nuclear environment. The direct streaming neutrons will pass through without impinging on the insulator. The insulator at the chamber wall is protected from the neutrons emitted from the target by the Flibe jets. The impact of lithium enrichment on improving the shielding performance is minimal. The results imply that using 65 cm thick jet assemblies provides adequate shielding for the insulator units.

The ion beam final focusing system is located at 10 m from the plasma adiabatic lens. Four superconducting coils surround the four ion beam tubes. Additional shielding is needed to protect the magnets. The insulator dose limit was found to be the most limiting parameter that determines the shielding requirement. The results indicate that a shield with a thickness ranging between 45 and 90 cm needs to be provided in front of the quadrupole unit. The final laser mirrors located along the channel axis are in the direct line-of-sight of source neutrons. Neutronics calculations were performed to determine the constraints on the placement of these mirrors to be lifetime components.

Acknowledgments

This work was supported by the U.S. Department of Energy and Lawrence Berkeley National Laboratory.

References

[1] S. Yu et al., “Plasma-Channel-Based Reactor and Final Transport,” Nuclear Instruments and Methods in Physics Research, 415 (1998) 174-181.

[2] R.W. Moir et al., “HYLIFE-II: A Molten-Salt Inertial Fusion Energy Power Plant Design-Final Report,” Fusion Technology, 25 (1994) 5-25.

[3] L.J. Perkins, “Materials Considerations for Highly Irradiated Normal-Conducting Magnets in Fusion Reactor Applications,” J. Nucl. Mater., 123, 1371 (1984).

[4] F. Clinard, “Ceramics for Applications in Fusion Systems,” J. Nucl. Mater., 85&86, 393 (1979).

[5] G. Hurley et al., “Structural Properties of MgO and $MgAl_2O_4$ After Fission Neutron Irradiation Near Room Temperature,” LA-UR 81-2078, Los Alamos National Laboratory (1981).

[6] L.J. Perkins, “Radiation Dose-Rate Resistivity Degradation in Ceramic Insulators and Assessment of the Consequences in Fusion Reactor Applications,” UWFDM-469, Fusion Technology Institute, University of Wisconsin (1982).

[7] Technical Basis for the ITER Interim Design Report, Cost Review and Safety Analysis, ITER EDA Documentation Series, No. 7, International Atomic Energy Agency, Vienna, April 1996.

[8] M. Sawan and P. Walstrom, “Superconducting Magnet Radiation Effects in Fusion Reactors,” Fusion Technology, 10/3, 741 (1986).

[9] M.E. Sawan, W.F. Vogelsang and D.K. Sze, “An Effective Penetration Shield Design for ICF Reactors,” Proc. 6th International Conf. on Radiation Shielding, Tokyo, Japan, 16-20 May 1983, pp. 675.

[10] R.L. Bieri and M.W. Guinan, “Grazing Incidence Metal Mirrors as the Final Elements in a Laser Driver for Inertial Confinement Fusion,” Fusion Technology, 19, 673 (1991).